International Journal of Energy
ISSN: 2957-9473 | Vol. 10, No. 3, 2026

Graded Diagnosis of 110 kV Porcelain Insulator Degradation based on Spatial Electric Field Distribution

Jiong Liu [1, *], Ming Liang [1], Huan Tang [1], Yongsheng Wang [2], Le Yang [2]

[1] Southwest Electric Power Design Institute Co., Ltd. of China Power Engineering Consulting Group, Chengdu, Sichuan, 610056, China
[2] Xi'an Jiaotong University, Xi'an, Shaanxi, 710049, China

*** Corresponding author:** Jiong Liu

Abstract: A graded diagnosis method for 110 kV porcelain insulator degradation is proposed based on spatial electric-field distribution. The study is limited to a seven-disc 110 kV porcelain suspension insulator string so that modeling, feature extraction, and validation remain focused on one practical operating scenario. First, a finite-element baseline model is built for the healthy 110 kV porcelain insulator string to obtain the axial electric-field distribution pattern. Second, continuous RMS samples acquired by an unmanned-aerial-vehicle-mounted all-fiber electric-field sensor are converted into electric-field intensity, interpolated, divided into seven adaptive segments, and represented by trimmed-mean disc-level features. Finally, a dual-index decision rule combining a dynamic-rate ratio and a standard-deviation ratio is developed, followed by a four-level disc degradation grading model. Laboratory experiments on 110 kV seven-disc strings show that the method can locate degraded discs and provide severity grades. In the tested cases, the recall is higher than 94.5%, the false alarm rate is below 5.5%, and a single analysis takes less than 15 s.

Keywords: Porcelain Insulator; Degradation Diagnosis; Spatial Electric Field; All-fiber Electric-field Sensor.

1. Introduction

Porcelain insulators in 110 kV transmission lines are exposed to electric stress, pollution, moisture, temperature cycling, and mechanical loading. Local degradation, low-value discs, or zero-value discs may distort the electric-field distribution and increase the risk of flashover. Manual inspection and image-based inspection provide effective solutions for visible defects, while electrical indicators such as leakage current have also been investigated for insulator condition monitoring [1]. Unmanned aerial vehicles (UAVs) have also been widely adopted for autonomous porcelain insulator inspection using aerial imaging techniques in distribution systems [2].

In field inspection, degradation of a porcelain disc is not always accompanied by visible surface damage. A disc may remain visually intact while its insulation resistance decreases or its dielectric state becomes abnormal. In this case, the degraded disc bears a lower voltage share and the electric field of adjacent discs is redistributed. Relying only on appearance images or manual experience may therefore lead to missed detections, while offline testing is difficult to apply frequently to energized transmission corridors.

Electric-field detection provides a non-contact electrical indicator. Recent studies have further demonstrated the feasibility of using spatial electric-field variation and UAV-mounted electric-field sensors for zero-value insulator detection [3]. A healthy seven-disc 110 kV porcelain string exhibits a smooth axial electric-field profile, while degradation in one disc produces a local distortion and an abnormal gradient between neighboring discs. This phenomenon has also been experimentally observed in live-line electric-field detection of deteriorated insulators[4].This property makes electric-field distribution suitable for disc-level diagnosis.

Existing electric-field-based monitoring methods have been used to characterize porcelain-insulator conditions under different operating or contamination states[5]. Although this approach is simple, it does not fully consider the natural position-dependent field distribution along a seven-disc string. For a 110 kV porcelain string, the high-voltage end, middle discs, and grounded end have different baseline field levels. Applying one absolute threshold to all positions may cause false alarms at naturally high-gradient positions or miss a local low-value disc.

This paper focuses only on the 110 kV porcelain suspension-insulator case. The contribution is a compact diagnosis workflow that combines a 110 kV porcelain electric-field baseline model, disc-level feature extraction from UAV-borne all-fiber sensor data, a dual-index degradation decision rule, and severity grading for maintenance support. The main idea is to establish a healthy position-specific baseline first, then convert the measured curve into adjacent-disc dynamic rates, and finally identify degradation using both relative amplification and statistical deviation.

2. Porcelain Electric-field Baseline

Modeled as the diagnostic object. The string is represented by cap-and-pin porcelain units, metal caps and pins, and the surrounding air domain. The detection distance is set to 60 cm according to the intended UAV inspection geometry.

Finite-element simulation is performed using an electrostatic model. The finite-element method has been widely applied to analyze the influence of porcelain insulator deterioration on axial electric-field distribution and voltage sharing characteristics[6-7]. A 110 kV-class energized-end boundary and a 0 V grounded-end boundary are used to represent the operating voltage class considered in this study. Air, metal fittings, and porcelain are assigned material

parameters. Mesh refinement is applied around shed edges, cap-pin interfaces, and metal fittings, where the electric-field gradient is high. Finite-element electric-field analysis has also been applied to evaluate porcelain-insulator performance under different environmental conditions[8].

The baseline model is not intended to replace field measurement; rather, it provides a position-related healthy reference. Because the voltage sharing of each porcelain disc is different, the field curve of a healthy string is inherently non-uniform. The non-uniform electric-field distribution of porcelain insulators is also affected by their geometry and surrounding conditions[9]. After this non-uniformity is included in the baseline, the diagnosis changes from judging whether an absolute field value is high or low to judging whether the same disc position deviates abnormally from its healthy reference.

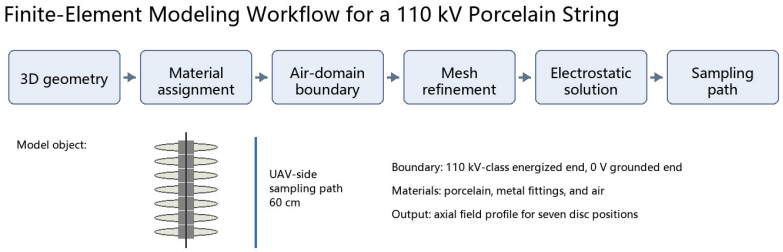

Fig 1. Finite-element modeling workflow for the 110 kV porcelain insulator string

Table 1. 110 kV baseline model configuration

Object	Structure	Purpose
Porcelain string	Seven-disc cap-and-pin suspension string	Healthy baseline for disc-level field comparison
Single disc	Porcelain body with metal cap and pin	Local distortion analysis under disc degradation
Air domain	UAV-side detection path at 60 cm	Spatial sampling path for field-feature extraction

The simulated healthy profile shows a middle-high and end-low axial trend along the porcelain string. Therefore, the diagnostic threshold should be referenced to disc position instead of using a universal absolute field-deviation threshold. When one porcelain disc deteriorates, its equivalent insulation capability decreases, and the local potential distribution and field gradient between adjacent discs change accordingly. This mechanism provides the physical basis for the subsequent dynamic-rate criterion.

Considering that UAV measurement may include slight attitude swing and path deviation, this study does not use a single field point as the diagnostic variable. Environmental conditions such as suspended particles can also introduce distortions into the electric-field distribution of porcelain insulators[10]. Instead, a spatial sequence is extracted along the axial sampling path. This representation preserves the local distortion caused by degradation while allowing segment-level statistics to suppress occasional sampling errors.

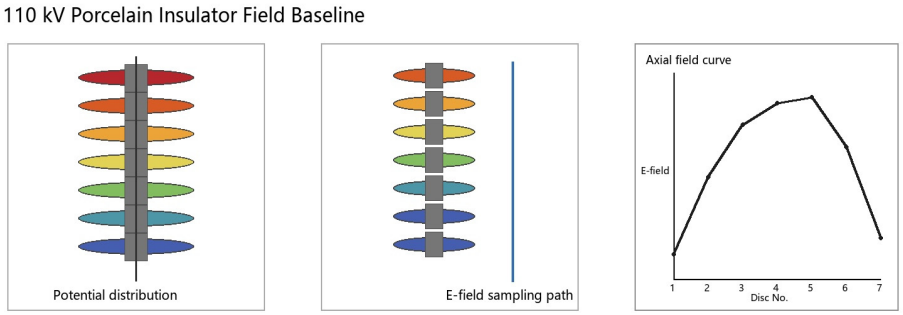

Fig 2. Simulated electric-field distribution of the 110 kV porcelain insulator string

3. Diagnosis Method

(1) Disc-Level Feature Extraction

Fiber-optic electric-field sensing has been demonstrated as a promising dielectric approach for contactless insulator condition monitoring [11]. The sensor output is received as a continuous RMS stream. Valid RMS values are parsed from the serial data and converted to electric-field intensity. The sequence is interpolated to reduce the influence of non-uniform sampling caused by flight speed variation.

Because the target object is a seven-disc 110 kV string, the electric-field sequence is adaptively divided into seven segments. Each segment corresponds to one disc. The representative feature of each segment is calculated using a trimmed mean, where the maximum and minimum samples are removed before averaging. This reduces the influence of transient UAV vibration and sensor outliers.

The processing chain consists of valid-frame screening, outlier removal, spatial interpolation, and disc-position mapping. Valid-frame screening removes communication interruptions or abnormal data frames. Outlier removal suppresses instantaneous sensor spikes. Spatial interpolation converts the non-equidistant sampling sequence into an approximately uniform axial sequence. Disc-position mapping then assigns the samples to the seven physical disc intervals of the porcelain string.

The trimmed mean is adopted instead of the ordinary mean because a UAV platform may be affected by wind disturbance, attitude correction, and local electromagnetic fluctuation during close inspection. Removing the maximum and minimum samples in each segment makes the retained samples more representative of the stable field level around

that disc, improving feature repeatability across repeated measurements.

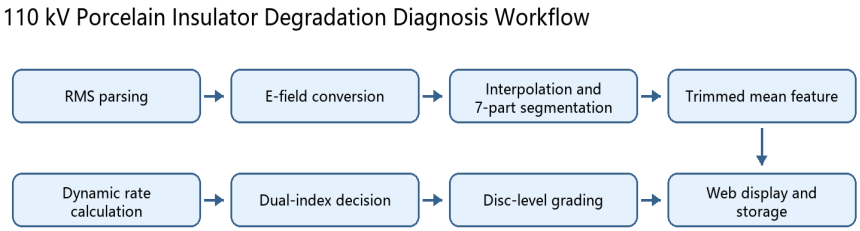

Fig 3. Proposed workflow for 110 kV disc-level degradation diagnosis

(2)Dual-Index Decision Rule

Let E1,E2,...,E7 denote the extracted disc-level field features. The dynamic electric-field change rate of the i-th disc is defined as dE_rate(i)=|E(i)-E(i-1)|/E(i-1)*100%, i=2,...,7. This index captures local field-gradient changes along the string.

The dynamic-rate ratio Rratio(i) is defined as the ratio between the tested string and the healthy baseline at the same disc position. If Rratio(i)>1.5, the disc is identified as degraded. To capture statistically significant deviations, a second index Rstd(i)=|dE_test(i)-mu0(i)|/sigma0(i) is introduced, where mu0(i) and sigma0(i) are the mean and standard deviation of the healthy dynamic rate at the same disc position. If Rstd(i)>2, the disc is also identified as degraded. The two conditions are combined with OR logic.

The dual-index design balances engineering interpretability and statistical robustness. Recent studies have also combined electric-field-related indicators with machine-learning classifiers for porcelain-insulator condition assessment[12]. Rratio describes the amplification of the measured local gradient relative to the healthy baseline, which is convenient for threshold setting and field explanation. Rstd measures whether the deviation exceeds the normal fluctuation range of the same position. When either index exceeds its threshold, the disc is marked as a suspected degraded disc and passed to the grading stage.

Compared with direct comparison of field amplitude, the dynamic-rate feature emphasizes the relative variation between adjacent discs. This helps reduce the influence of overall voltage fluctuation, slight distance variation, and environmental background change. For a 110 kV porcelain string, the adjacent-disc relationship is also consistent with voltage redistribution caused by local low-value degradation, so the indicator has clear physical meaning.

(3) Four-Level Grading

Table 2. Disc-level degradation rule

Grade	Condition	Maintenance meaning
Normal	Rratio <= 1.5	Routine inspection
Slight	1.5 < Rratio <= 2.5	Shorten inspection interval
Moderate	2.5 < Rratio <= 4.0	Schedule targeted verification
Severe	Rratio > 4.0	Replace the degraded disc as soon as practical

The grading result is intended to support maintenance decisions rather than only giving a binary normal/abnormal output. Slight degradation can be recorded as a tracking target for the next inspection cycle. Moderate degradation should be verified together with infrared inspection, offline testing, or historical defect records. Severe degradation should be prioritized for disc replacement. In this way, the electrical diagnosis result can be connected with defect closed-loop management. These four grades represent diagnostic severity levels defined by the proposed electric-field indicators rather than direct measurements of insulation resistance or naturally aged degradation severity.

4. Experimental Verification

All tests are conducted in a controlled laboratory environment using seven-disc 110 kV cap-and-pin porcelain suspension insulator strings. Four degradation grades (Normal, Slight, Moderate, Severe) are simulated by artificially short-circuiting individual discs with varied external resistors to mimic insulation resistance drop and zero-value faults. All measurement data are derived from lab-controlled simulated tests rather than naturally aged field insulators. The applied test voltage is 63.5 kV (phase-to-ground rated voltage for 110 kV systems), with clean insulator surfaces. The all-fiber electric-field sensor is calibrated against a standard high-voltage probe to establish the RMS-to-field-intensity conversion. The nominal detection distance is fixed at 60 cm, consistent with the baseline model.

The validation uses 110 kV seven-disc porcelain insulator strings under healthy and degraded conditions. The fixed-threshold method uses a uniform 3% field-deviation threshold, while the proposed method uses baseline-referenced dynamic rates and statistical deviation. This design avoids applying the same absolute threshold to all disc positions.

The verification follows the sequence of healthy-baseline acquisition, degraded-sample acquisition, feature extraction, disc-position decision, and grade output. Healthy samples are used to determine the reference dynamic rate and fluctuation range of each disc position. Degraded samples are then used to test whether the algorithm can identify the correct disc number at the position where local curve distortion appears. To stay close to UAV inspection practice, the complete processing chain from RMS parsing to web-based result display is retained.

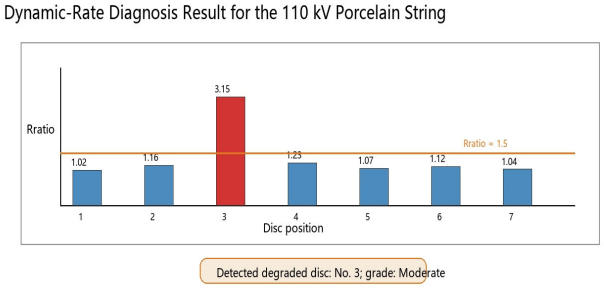

Fig 4. Dynamic-threshold diagnosis results for the 110 kV porcelain case

The healthy curves show smooth axial distributions, whereas the degraded case presents a local distortion around

the degraded disc. The proposed method maps this distortion to the corresponding disc number and outputs the degradation grade. The web interface stores RMS value, electric-field intensity, dynamic rate, degradation mark, and disc number for traceability.

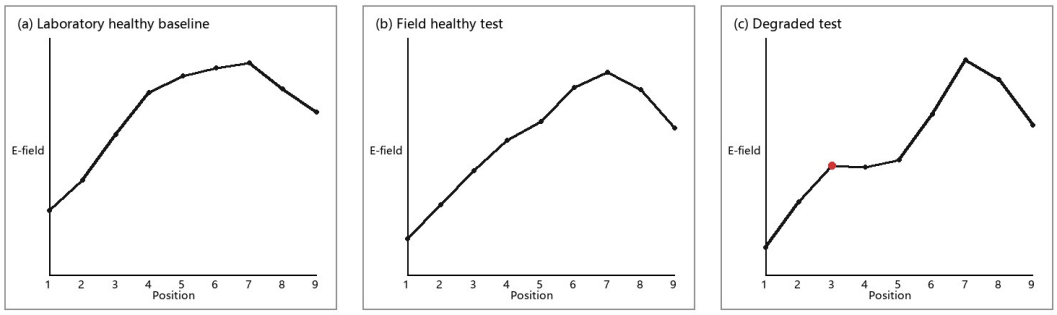

Fig 5. Healthy and degraded electric-field curves of 110 kV seven-disc porcelain strings

Table 3. Comparison of diagnosis strategies for the 110 kV case

Diagnosis strategy	Basis	Main limitation or effect
Fixed threshold	Field deviation > 3%	Simple but sensitive to disc position and environmental fluctuation
Dynamic interval	Adjacent-disc rate outside normal range	Improves position adaptation but lacks severity grading
Proposed method	Rratio>1.5 or Rstd>2 with Rratio grading	Disc-level localization and four-level severity grading; recall >94.5%, false alarm <5.5%

The comparison indicates that the fixed-threshold method is sensitive to the natural field difference between end and middle positions. A low threshold increases false alarms, while a high threshold may miss a low-value disc. The dynamic-interval method improves position adaptability, but without severity grading it is still insufficient for maintenance priority ranking. The proposed method provides disc localization and four-level severity output, making it more suitable for automatic screening and inspection-data management. Due to the limited sample-level records available for this laboratory validation, the present study reports overall recall and false-alarm rate rather than class-wise precision, recall, F1-score, and confusion matrix. Class-wise statistical evaluation and repeated-measurement uncertainty analysis will be included in subsequent validation with expanded sample-level measurements.

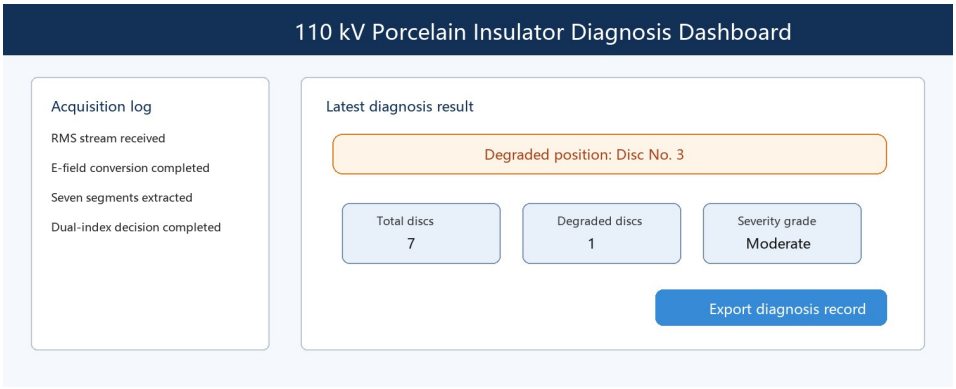

Fig 6. Web display of the graded degradation diagnosis result

5. Conclusion

A graded degradation diagnosis method for 110 kV porcelain insulator strings has been presented. The method uses a finite-element electric-field baseline for a seven-disc porcelain string, converts UAV-borne all-fiber sensor measurements into seven disc-level field features, and applies a dual-index decision rule for degradation detection.

Validation results verify accurate disc localization and four-level severity grading under controlled laboratory conditions. Note that on-site diagnosis performance may decline due to field environmental interferences, as all indicators are obtained in stable lab settings. Compared with the fixed-threshold method, the position-referenced approach better compensates for axial electric-field differences and supports inspection, defect tracking and maintenance decisions.

Further field verification is needed. Key factors—humidity, contamination, insulator geometry and detection distance—will be systematically studied for their impacts on field distribution and measurement sensitivity. Future work will expand the test dataset, collect more field-degraded samples, refine grading thresholds and explore multi-inspection trend fusion.

References

[1] Salem, A. A., Lau, K. Y., Ishak, M. T., Abdul-Malek, Z., Al-Gailani, S. A., Al-Ameri, S. M., Mohammed, A., Alashbi, A. A. S., & Ghoneim, S. S. M. (2022). Monitoring porcelain insulator condition based on leakage current characteristics. Materials, 15(18), 6370. https://doi.org/10.3390/ma15186370.

[2] Rahman, E. U., Zhang, Y., Ahmad, S., Ahmad, H. I., & Jobaer, S. (2021). Autonomous vision-based primary distribution systems porcelain insulators inspection using UAVs. Sensors, 21(3), 974. https://doi.org/10.3390/s21030974.

[3] Zhang, Z., Zhang, H., Jiang, X., Zhou, C., Liu, R., & Li, Y. (2025). Detection of zero-value insulators in ±800 kV DC porcelain strings based on spatial electric field variation. Journal of Electrostatics, 138, 104206. https://doi.org/10.1016/j.elstat.2025.104206.

[4] Wu, S., Wang, L., Song, B., & Gao, J. (2024). Live-line detection of deteriorated insulators on overhead transmission lines based on electric field distribution. IEEE Sensors Journal, 24(2), 1687–1695. https://doi.org/10.1109/JSEN.2023.3332849.

[5] Zhang, D., Zhang, Y., Liu, H., Cheng, Y., Wan, W., Gao, T., Han, X., Zhang, Z., & Jiang, X. (2024). Research on the prediction method of porcelain insulator pollution degree based on electric field monitoring. Electric Power Systems Research, 233, 110488. https://doi.org/10.1016/j.epsr.2024.110488.

[6] Zhou, J., Li, X., Xu, Z., Zhu, Y., Li, X., & Ma, H. (2021). Influence of porcelain insulator deterioration on axial electric field distribution of transmission line insulator string based on finite element method. Insulating Materials, 54(10), 79–83. https://doi.org/10.16790/j.cnki.1009-9239.im.2021.10.012.

[7] Ghermoul, O., Benguesmia, H., & Benyettou, L. (2023). Finite element modeling for electric field and voltage distribution along the cap and pin insulators under pollution. Diagnostyka, 24(2), 1–9. https://doi.org/10.29354/diag/159517.

[8] Al-Karawi, S., & Al-Taie, A. (2024). Superhydrophobic coating for enhancing porcelain insulators performance under pollution conditions. e-Prime—Advances in Electrical Engineering, Electronics and Energy, 8, 100515. https://doi.org/10.1016/j.prime.2024.100515.

[9] Li, Y., Wu, H., Liu, S., Liu, X., Zhao, Y., Chen, R., & Yang, G. (2023). Effect of sand covering on surface electric field and potential distributions of 110 kV porcelain insulator. Insulating Materials, 56(5). https://doi.org/10.16790/j.cnki.1009-9239.im.2023.05.014.

[10] Li, Y., Yang, G., Wu, H., Kang, W., Xiang, Z., Liu, S., Zhang, J., & Zhao, Y. (2023). The variation law of surface potential and electric field of porcelain insulator in suspended sand and dust environment. Insulating Materials, 56(8), 87–93. https://doi.org/10.16790/j.cnki.1009-9239.im.2023.08.013.

[11] Ramnarine, V., Liu, F., Peesapati, V., & Djurović, S. (2026). Packaged FBG + PMN-PT sensor for contactless electric field monitoring of overhead line insulators. IEEE Sensors Journal, 26(7), 9851–9860. https://doi.org/10.1109/JSEN.2026.3661239.

[12] Salem, A. A., Al-Gailani, S. A., Amer, A. A. G., Alsharef, M., Bajaj, M., Zaitsev, I., Ngah, R., & Ghoneim, S. S. M. (2024). Classification of RTV-coated porcelain insulator condition under different profiles and levels of pollution. Scientific Reports, 14, 22759. https://doi.org/10.1038/s41598-024-73520-7.